

University of Nebraska - Lincoln
DigitalCommons@University of Nebraska - Lincoln

Mechanical & Materials Engineering Faculty
Publications

Mechanical & Materials Engineering, Department
of

2012

Thickness-shear and thickness-twist modes in an oblate elliptical ceramic cylinder and energy trapping in contoured acoustic wave resonators

Huijing He

University of Nebraska-Lincoln, he.hui.jing@hotmail.com


Jiashi Yang

University of Nebraska-Lincoln, jyang1@unl.edu

Yi-hua Huang

Sun Yat-sen University

Follow this and additional works at: <http://digitalcommons.unl.edu/mechengfacpub>

 Part of the [Mechanics of Materials Commons](#), [Nanoscience and Nanotechnology Commons](#), [Other Engineering Science and Materials Commons](#), and the [Other Mechanical Engineering Commons](#)

He, Huijing; Yang, Jiashi; and Huang, Yi-hua, "Thickness-shear and thickness-twist modes in an oblate elliptical ceramic cylinder and energy trapping in contoured acoustic wave resonators" (2012). *Mechanical & Materials Engineering Faculty Publications*. 226.
<http://digitalcommons.unl.edu/mechengfacpub/226>

This Article is brought to you for free and open access by the Mechanical & Materials Engineering, Department of at DigitalCommons@University of Nebraska - Lincoln. It has been accepted for inclusion in Mechanical & Materials Engineering Faculty Publications by an authorized administrator of DigitalCommons@University of Nebraska - Lincoln.

THICKNESS-SHEAR AND THICKNESS-TWIST MODES IN AN OBLATE ELLIPTICAL CERAMIC CYLINDER AND ENERGY TRAPPING IN CONTOURED ACOUSTIC WAVE RESONATORS

Hui-jing HE¹, Jia-shi YANG^{1,*}, Yi-hua HUANG²

¹Department of Mechanical and Materials Engineering, University of Nebraska-Lincoln, Lincoln, NE 68588-0526, USA

²Department of Electronic and Communication Engineering, Sun Yat-sen University, Guangzhou 510006, Guangdong, China

*Corresponding author, E-mail: jyang1@unl.edu; Tel.: 402-4720712.

We study shear-horizontal motions of a piezoelectric ceramic cylinder with an oblate elliptical cross section and axial poling. Exact thickness-shear and thickness-twist vibration modes are obtained. These modes show energy trapping, i.e., the vibration is mainly confined near the thick, central region and decays to almost nothing near the edges. The results are useful for the understanding and design of contoured piezoelectric resonators for strong energy trapping.

Keywords: Elliptic; Resonator; Energy trapping

1. INTRODUCTION

Shear vibration modes of crystal plates including face shear (FS), thickness shear (TSh), and thickness twist (TT) [1] are the modes used most often for bulk acoustic wave resonators and resonator-based sensors. An important aspect of these modes is their energy trapping behavior. In a partially electroded plate, TSh and TT vibrations are largely confined to the electroded central region of the plate [2], and fall off rapidly in amplitude outside of this region. Near the edges of the plate there is essentially no vibration and therefore the plate can be mounted at the edges without affecting its vibration. Analysis of the partially electroded plate has shown that the energy trapping is due to mass loading on the elastic plate by the electrodes [2]. Contoured plates with varying thickness (thick in the central region and thin near the edges) can also produce strong energy trapping [3]. Contoured piezoelectric resonators are widely used and energy trapping in these resonators has sustained research interest for many years. However, analyses to date have typically involved approximate solutions, and exact solutions are rare. Mathematically, the analysis of contoured resonators leads to partial differential equation over a complicated domain when using the three-dimensional equations of elasticity or piezoelectricity, or differential equations with variable coefficients when using the two-dimensional plate equations. This presents considerable mathematical challenges and usually various approximations need to be made to obtain a solution. Only in rare situations can exact modes be obtained. Recently, in a previous paper [4], we obtained exact TSh and TT modes in an isotropic

elastic cylinder with an oblate elliptical cross section which may be viewed as a contoured resonator. In this paper, we generalize the analysis in [4] from elastic to piezoelectric. We study SH vibrations in a piezoelectric cylinder of polarized ceramics with an oblate elliptical cross section.

2. GOVERNING EQUATIONS

Consider an elliptical cylinder of ceramics poled in the x_3 direction as shown in Fig. 1. The surface of the cylinder is traction free and is unelectroded. Effects of the electric field that may exist in the surrounding free space are known to be small and are neglected as usual.

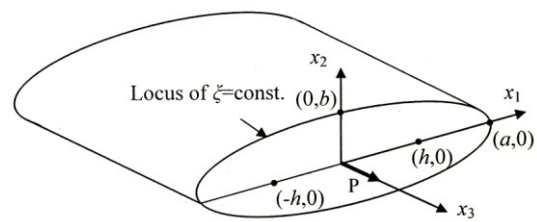


Figure 1. An elliptical cylinder of polarized ceramics

We are interested in shear-horizontal (SH) motion described by

$$u_1 = u_2 = 0, \quad u_3 = u_3(x_1, x_2, t), \quad \phi = \phi(x_1, x_2, t). \quad (1)$$

The nontrivial equation of motion and the charge equation of electrostatics governing u_3 and ϕ take the following form [5]:

$$c\nabla^2 u_3 + e\nabla^2 \phi = \rho \ddot{u}_3, \quad e\nabla^2 u_3 - \varepsilon \nabla^2 \phi = 0. \quad (2)$$

We introduce $\psi = \phi - (e/\varepsilon)u_3$ [5], then

$$v_T^2 \nabla^2 u_3 = \ddot{u}_3, \quad \nabla^2 \psi = 0. \quad (3)$$

Consider time-harmonic free vibrations for which all fields have the same $\exp(i\omega t)$ factor which will be dropped for simplicity. For such motions (3)₁ reduces to Helmholtz equation:

$$v_T^2 \nabla^2 u_3 = -\omega^2 u_3. \quad (4)$$

In elliptical coordinates defined by

$$x_1 = h \cosh \xi \cos \eta, \quad x_2 = h \sinh \xi \sin \eta, \quad (5)$$

(4) and (3)₂ take the following form [6]:

$$\frac{\partial^2 u_3}{\partial \xi^2} + \frac{\partial^2 u_3}{\partial \eta^2} + 2q(\cosh 2\xi - \cos 2\eta)u = 0, \quad (6)$$

$$\frac{\partial^2 \psi}{\partial \xi^2} + \frac{\partial^2 \psi}{\partial \eta^2} = 0. \quad (7)$$

3. SOLUTION PROCEDURE

For an unelectroded cylinder, the charge-free boundary condition takes the form of $\partial\psi/\partial\xi=0$. This, together with (7), shows that ψ is determined by the second boundary-value problem of Laplace equation with a homogeneous boundary condition. From the uniqueness theorems of Laplace equation it can be concluded that in this case ψ is no more than a constant which can be taken to be zero. In this case ϕ is proportional to u_3 . The electric field (potential gradient) is proportional to strain (displacement gradient).

By the method of separation of variables in partial differential equations, we write u_3 as:

$$u_3(\xi, \eta) = U(\xi)V(\eta). \quad (8)$$

Substitution of (8) into (4) results in the following two ordinary differential equations:

$$\frac{d^2 V(\eta)}{d\eta^2} + (\lambda - 2q \cos(2\eta))V(\eta) = 0, \quad (9)$$

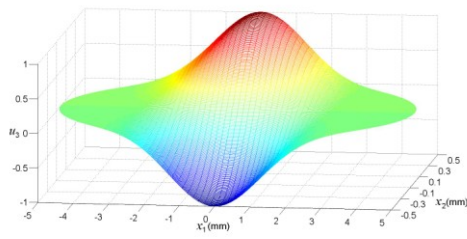
$$\frac{d^2 U(\xi)}{d\xi^2} + (2q \cosh(2\xi) - \lambda)U(\xi) = 0, \quad (10)$$

where λ is a separation constant. (9) and (10) are

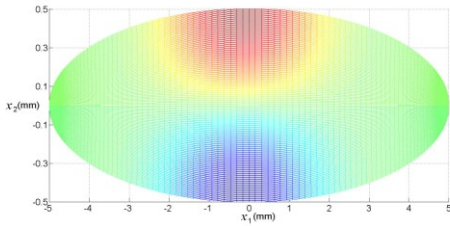
known as the angular and radial Mathieu equations, respectively. There are systematic theoretical results for the solutions of these equations [6] and how to calculate them. They are complicated and therefore are not presented here. More details can be found in [4].

4. NUMERICAL RESULTS

As a numerical example, consider a cylinder made of polarized ceramics PZT-4. $a=5$ mm and $b=0.5$ mm except in Fig. 5 below. The fundamental TSh mode is the one most widely used in acoustic wave devices. The displacement distribution of this mode over a cross section is shown in Fig. 2. In the figure, the semi-major and semi-minor axes a and b are not drawn to scale. This mode has one nodal line with zero displacement at $x_2=0$ or along the x_1 axis. When the upper half of the cross section is moving in one direction, the lower half moves in the opposite direction. Although the top and bottom of the cylinder are moving with the largest displacement, the left and right edges are essentially not moving. This is the so-called energy trapping phenomenon. With energy trapping, the cylinder can be mounted at the left and/or right edges without affecting the vibration in the central region. To quantify energy trapping, we introduce an X which is determined by that the central portion of the cross section with $|x_1| < X$ carries 90% of the vibration energy. The electric potential distribution is proportional to the displacement distribution in Fig. 2. Figs. 3 and 4 show the strain distributions of the fundamental TSh mode which are proportional to the electric field distributions.

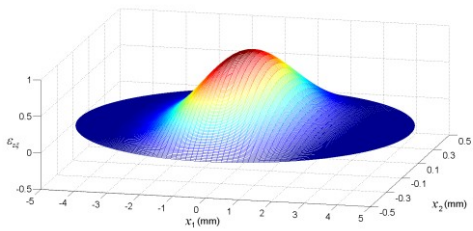


(a)

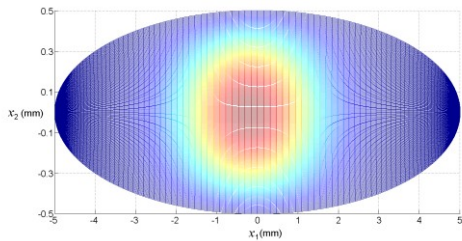


(b)

Figure 2. Displacement distribution of the fundamental TSh mode. $\omega=8.4086192 \times 10^6$ rad/s. $X=1.088$ mm. (a) 3-D view. (b) 2-D view.

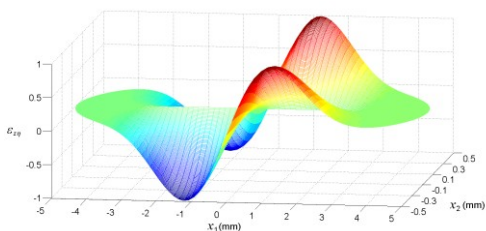


(a)

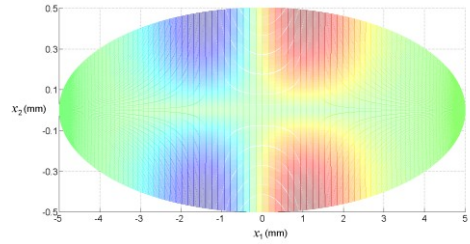


(b)

Figure 3. Distribution of the strain component ϵ_{zz} of the fundamental TSh mode.



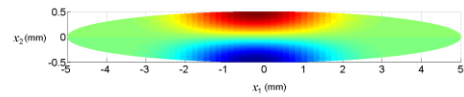
(a)



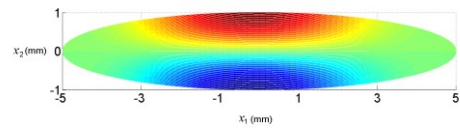
(b)

Figure 4. Distribution of the strain component $\epsilon_{z\eta}$ of the fundamental TSh mode.

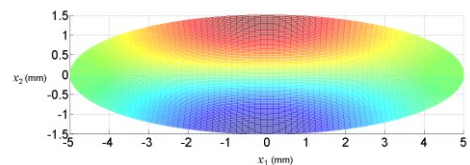
Fig. 5 shows the effect of b/a on the fundamental TSh mode. It is drawn to scale. a is fixed and b varies. It can be seen that as b increases, the displacement distribution becomes wider or is less trapped.



(a)



(b)



(c)

Figure 5. Effect of b/a on the fundamental TSh mode.

Fig. 6 shows two higher-order TSh modes. They have two and three nodal lines roughly parallel to the x_1 axis, respectively. They may be symmetric or antisymmetric about the x_1 axis. The frequencies of the modes in Fig. 2 and Fig. 6 are roughly equally spaced although not exactly so. Clearly, higher-order modes are better trapped, i.e., with narrower vibration distributions in the x_1 direction.

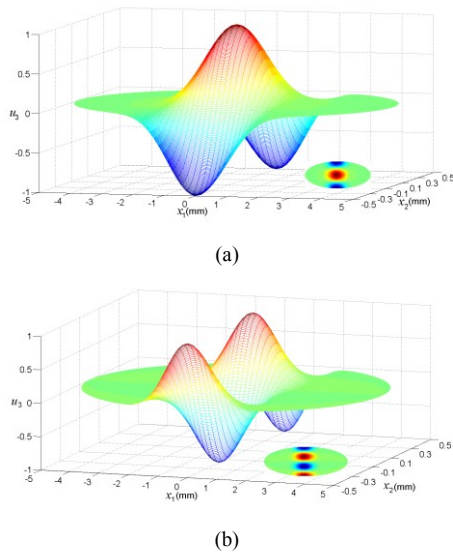


Figure 6. Higher-order TSh modes.
 (a) $\omega=1.6570726 \times 10^7$ rad/s. $X=0.783$ mm.
 (b) $\omega=2.4729652 \times 10^7$ rad/s. $X=0.626$ mm.

Corresponding to the fundamental TSh mode in Fig. 2 with a nodal line at $x_2=0$, there are higher-order modes with additional roughly vertical nodal lines as shown in Fig. 7 (a) and (b) with an increasing number of one and two vertical nodal lines, respectively. These are TT modes. The figures show that higher-order TT modes are trapped less. Unlike the nearly harmonic frequencies of the TSh modes in Figs. 2 and 6, the frequencies of the TT modes in Fig. 7 (a) and (b) increase only slightly. More complicated modes can be found in [4].

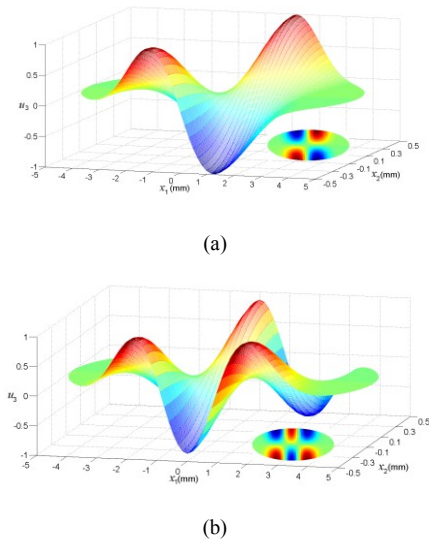


Figure 7. TT modes.
 (a) $\omega=8.9436549 \times 10^6$ rad/s. $X=1.834$ mm.
 (b) $\omega=9.4939179 \times 10^6$ rad/s. $X=2.263$ mm.

5. CONCLUSION

Exact solutions for SH modes are obtained for an oblate piezoelectric elliptical cylinder. TSh and TT modes show energy trapping. Higher-order TSh modes exhibit rapidly increasing (nearly harmonic) frequencies and better energy trapping. Higher-order TT modes have slowly increasing frequencies and are less trapped. Flatter ellipses with smaller values of b/a have stronger energy trapping. For an unelectroded cylinder, the electric potential is proportional to the displacement, and the electric field is proportional to the strain. The case of an electroded cylinder remains challenging.

ACKNOWLEDGEMENTS

The authors gratefully acknowledge the financial support of this research by the National Natural Science Foundation of China under Grant 60871059, 61172025 and the Fundamental Research Funds for the Central Universities under Grant 11lgpy35. This work was also partially supported by the US Army Research Office under DAAD19-01-1-0443.

REFERENCES

- [1] Mindlin RD. *An Introduction to the Mathematical Theory of Vibrations of Elastic Plates*. Yang JS, ed., World Scientific, Singapore, 2006.
- [2] Mindlin RD, Lee PCY. Thickness-shear and flexural vibrations of partially plated, crystal plates. *Int. J. Solids Structures* **2**(1): 125-139, 1966.
- [3] Mindlin RD, Forray M. Thickness-shear and flexural vibrations of contoured crystal plates. *J. Appl. Phys.* **25**(1): 12-20, 1954.
- [4] He HJ, Yang JS, Kosinski JA. Shear-horizontal vibration modes of an oblate elliptical cylinder and energy trapping in contoured acoustic wave resonators. *IEEE Trans. Ultrason., Ferroelect., Freq. Contr.* **59**(8): 1774-1780, 2012.
- [5] Bleustein JL. Some simple modes of wave propagation in an infinite piezoelectric plate. *J. Acoust. Soc. Am.* **45**(3): 614-620, 1969.
- [6] McLachlan NW. *Theory and Application of Mathieu Functions*. Oxford Press, Oxford, 1951.